Environmental Microbiology
September 2014, Volume 16, Issue 9, pages 2777–2790
http://dx.doi.org/10.1111/1462-2920.12324

Bacterial communities and syntrophic associations involved in anaerobic oxidation of methane process of the Sonora Margin cold seeps, Guaymas Basin

Adrien Vigneron[1,2,3], Perrine Cruaud[1,2,3], Patricia Pignet[1,2,3], Jean-Claude Caprais[4], Nicolas Gayet[4], Marie-Anne Cambon-Bonavita[1,2,3], Anne Godfroy[1,2,3], Laurent Toffin[1,2,3,*]

[1] Ifremer, Laboratoire de Microbiologie des Environnements Extrêmes, Technopôle Brest Iroise, Plouzané, France
[2] Université de Bretagne Occidentale, Technopôle Brest Iroise, Plouzané, France
[3] CNRS, Laboratoire de Microbiologie des Environnements Extrêmes, Technopôle Brest Iroise, Plouzané, France
[4] Ifremer, Laboratoire Etude des Environnements Profonds, Technopôle Brest Iroise, Plouzané, France

*: Corresponding author : Laurent Toffin, tel. (+33) 2 98 22 43 96 ; fax (+33) 2 98 22 47 ;
email address : laurent.toffin@ifremer.fr

Abstract:

The Sonora Margin cold seeps present on the seafloor a patchiness pattern of white microbial mats surrounded by polychaete and gastropod beds. These surface assemblages are fuelled by abundant organic inputs sedimenting from the water column and upward-flowing seep fluids. Elevated microbial density was observed in the underlying sediments. A previous study on the same samples identified anaerobic oxidation of methane (AOM) as the potential dominant archaeal process in these Sonora Margin sediments, probably catalysed by three clades of archaeal anaerobic methanotrophs (ANME-1, ANME-2 and ANME-3) associated with bacterial syntrophs. In this study, molecular surveys and microscopic observations investigating the diversity of *Bacteria* involved in AOM process, as well as the environmental parameters affecting the composition and the morphologies of AOM consortia in the Sonora Margin sediments were carried out. Two groups of *Bacteria* were identified within the AOM consortia, the *Desulfosarcina/Desulfococcus* SEEP SRB-1a group and a *Desulfobulbus*-related group. These bacteria showed different niche distributions, association specificities and consortia architectures, depending on sediment surface communities, geochemical parameters and ANME-associated phylogeny. Therefore, the syntrophic AOM process appears to depend on sulphate-reducing bacteria with different ecological niches and/or metabolisms, in a biofilm-like organic matrix.

1. Introduction

The cold seeps of the Guaymas Basin, located along a transform fault of the Sonora Margin, present different faunal assemblages (Simoneit *et al*., 1990; Paull *et al*., 2007) and white microbial mats (Vigneron *et al*., 2013). The development of these communities at the cold seep water-sediment interface is supported by methane and sulphide-rich up-flowing fluids, and by seep-fuelled active methanogens and anaerobic methanotrophs (Boetius *et al*., 2000; Jorgensen and Boetius, 2007). Archaeal anaerobic methanotrophs (ANME-1, ANME-2a, ANME-2c and ANME-3), distantly related to the orders *Methanosarcinales* and *Methanomicrobiales* (Orphan *et al*., 2002; Knittel and Boetius, 2009), and probably involved in anaerobic oxidation of methane (AOM), have been found to be dominant in the shallow (0

to 17 cmbsf) Sonora Margin cold seep sediments (Vigneron et al., 2013). ANME clades presented different distributions throughout these sediments. In sediments underlying two visible microbial mats, called White Mat 12 (WM12) and White Mat 14 (WM14) (Supplementary Figure 1), ANME-2c were predominant in shallow sulfate-rich sediments while ANME-1 dominated the deepest sulfate-depleted sediment layers and ANME-3 were restricted to a specific horizon below the first 4 cm of sediments (Figure 3). ANME communities appeared to be favored in sulfate enriched sediments throughout sediment core WM12. Elsewhere, sulfate and methane porewater concentration profiles in sediments underlying macrofauna at the edge of WM14 (called EWM14), were similar to those found in sediments underlying microbial mats. However, in EWM14 sediment core, ANME-2c were restricted to the first sediment layers, while increasing population of ANME-1 appeared to be the sole ANME community in the deepest sediment layers (Figure 3). These ANME lineages are differently associated with syntrophic bacteria, depending on their phylogenetic affiliation and the environmental conditions. In the Sonora Margin sediments, ANME-2a and -2c were always observed forming aggregates with bacteria, whereas ANME-1 formed tight associations with bacteria exclusively in sulfate-rich sediments of WM12, and ANME-3 were observed without bacterial partners. Previous studies indicated that such syntrophic relationship between ANME and bacterial partners, mainly affiliated with sulfate-reducing *Bacteria* (SRB), linked AOM and seawater sulfate reduction in archaeal/bacterial consortia (Orphan et al., 2002; Knittel et al., 2005; Niemann et al., 2006; Pernthaler et al., 2008; Knittel and Boetius, 2009; Schreiber et al., 2010; Schubert et al., 2011). The sulfate-reducing *Bacteria,* affiliated to the *Deltaproteobacteria* (Knittel et al., 2003), form a large and diverse physiological group capable of degrading a wide range of organic and hydrocarbon-derived substrates (Dhillon et al., 2003; Kniemeyer et al., 2007), resulting in elevated sulfate reduction rates in cold seep sediments (Bowles et al., 2011). To date, only four phylogenetic clusters were observed in AOM consortia from cold seeps : the two *Desulfobulbus*-related organism groups (Losekann et al., 2007; Pernthaler et al., 2008), the SEEP SRB1a subgroup belonging to the *Desulfosarcina/Desulfococcus* group (DSS) (Boetius et al., 2000; Knittel et

al., 2003; Schreiber et al., 2010) and recently, the previously described group SEEP SRB-2 (Knittel et al., 2003; Kleindienst et al., 2012). Additionally, another deltaproteobacterial group, the Hotseep-1 cluster, was observed in ANME-1 consortia in the hydrothermal sediments of the Guaymas Basin (Holler et al., 2011). However, other unidentified *Bacteria* have been observed using direct cell capture experimentation (Pernthaler et al., 2008), and AOM has been demonstrated to be coupled with other metabolisms than sulfate reduction, such as iron, manganese or nitrate reduction (Raghoebarsing et al., 2006; Beal et al., 2009). Although these findings have led to the description of the AOM-driving and denitrifying bacteria *Candidatus Methylomirabilis oxyfera* (Ettwig et al., 2010), these results demonstrated that the diversity of AOM bacterial partners still needs to be completed. Furthermore, the ecophysiology of AOM-involved *Bacteria* and the exact mechanisms of this syntrophic association remain unclear. For example the vertical distribution and the metabolic specificities of each bacterial partner in the sediments are poorly explored. In this study, we focused on unexplored bacterial communities of the Sonora Margin cold seep sediments and more particularly on *Bacteria* involved in AOM. The identity and distribution of active bacterial communities involved in AOM were studied using complementary phylogenetic, microscopic and quantitative analyses in conjunction with a previous molecular survey on archaeal communities and geochemical analyses (Vigneron et al., 2013).

Results

Phylogenic diversity of metabolically active Bacteria

A total of 658 RNA-derived bacterial sequences were analyzed from the sediments underlying two white microbial mats (WM12, a thick mat harboring elevated sulfate concentrations throughout the sampled sediments and WM14, an extended mat surrounding a visible fluid output), and the edge of WM14 (EWM14) colonized by macrofauna. Bacterial diversity was high in the 16S rRNA clone libraries (Simpson indexes:1-$H_{Simpson}$ = 0.9±0.05), with more than 27 phylogenetic lineages, mainly distributed among the Epsilon, Delta and

Gammaproteobacterial groups (Figure 1 and Supplementary Material Figure 2). The number of sequences related to the *Epsilonproteobacteria,* and particularly affiliated to the *Sulfurovum* genus encompassing sulfur- and thiosulfate-oxidizers bacterium (Inagaki et al., 2004), decreased with depth. The *Deltaproteobacteria* represented about a third of analyzed sequences in WM12, WM14 and EWM14 sediment cores. The *Deltaproteobacteria* sequences were composed of diverse phylogenetic lineages (Figure 2), including the known AOM-associated sulfate-reducing bacterial groups such as the *Desulfosarcina/Desulfococcus* group (SEEP SRB-1a-f) (Schreiber et al., 2010) and SEEP SRB groups (SRB-2, -3 ,-4) (Knittel et al., 2003). SEEP SRB-1a were detected throughout the WM12 sediment core, in the middle (4-6 cmbsf) and bottom sediment layers of WM14 and only in the EWM14 surface sediment layer. In contrast, SEEP SRB1b were only detected in the deepest sediment layers of EWM14. The syntrophic AOM partners within the family *Desulfobulbaceae*, previously described from mud volcano sediments (Losekann et al., 2007), were detected throughout WM sediments and in higher proportion in core WM12. In contrast, in EWM14, *Desulfobulbus*-related sequences were only detected in the surface and middle sediment layers. SEEP SRB-2 sequences were detected in the deepest layers of WM12 and in higher proportion in EWM14 intermediate and deeper sediment layers. Sequences related to *Gammaproteobacteria,* previously detected in hydrocarbon rich environments, were also found in high proportion in WM14 sediments and from 0 to 6 cmbsf in EWM14. Sequences related to the *Candidatus Maribeggiatoa* genus were found in the first centimeters of the WMs (WM14 and WM12) sediments, as well as in dominant proportion in the microbial mats themselves. Additionally, sequences related to uncultured bacterial candidate division JS1 were only detected in the deepest sediment layers of EWM14, that was not covered by microbial mats. Finally, sequences affiliated to several groups of candidate divisions, *Bacteroidetes, Spirochaetes, Actinobacterium, Acidobacterium, Chloroflexi* and *Verrucomicrobia* were also detected in all samples in lower proportions (Figure 1 and Supplementary Figure 2).

Real-time PCR quantification of AOM bacterial partners

DSS, DBB, SEEP-SRB2 and JS1 abundances were estimated by real-time PCR every two centimeters from the water-sediment interface to 15 cmbsf (core length). These quantifications, targeting previously observed or suspected AOM-involved *Bacteria* (Losekann et al., 2007; Cambon-Bonavita et al., 2009; Harrison et al., 2009; Knittel and Boetius, 2009; Schreiber et al., 2010; Kleindienst et al., 2012), highlighted significant differences between microbial lineage distributions within each habitat. (One-way ANOVA; for WM12, $P < 0.01$; WM14, $P < 0.01$; EWM14, $P < 0.01$) (Figure 3). Overall, DSS members were the dominant SRB, as previously reported in other cold seep environments (Kniemeyer et al., 2007; Schreiber et al., 2010). SRB-related 16S rDNA copies were more abundant in WM12 sediments (4.52 x10^9 16S rDNA copies g^{-1}) where sulfate concentrations were high (22 to 13 mM). Significant differences in DBB and DSS depth distributions were also detected between the habitats (One-way ANOVA; for DSS, $P < 0.01$; DBB, $P < 0.01$). The number of DBB-related 16S rDNA copies increased with depth in WM12 and WM14 sediment cores, reaching a maximum of 2x10^9 16S rDNA copies g^{-1} of sediment around 6 to 10 cmbsf in WM12 and 5x10^8 copies g^{-1} in the 4-6 cmbsf WM14, then decreased deeper in the sediment. DBB 16S rDNA copy number was high (7.8x10^8 copies g^{-1}) in the first EWM14 sediment layers and then decreased with depth (1.2x10^7 copies g^{-1} in the bottom of the core) (Figure 3). DSS 16S rDNA copy number in WMs increased with depth until 6 cmbsf, reaching 2.6x10^9 and 6x10^8 copies g^{-1} in WM12 and WM14 respectively, then were fairly constant in the underlying sediment layers. However, in EWM14 sediments, DSS 16S rDNA copy numbers were high (5.8x10^8 copies g^{-1}) in the surface sediment layers (0-4 cmbsf) then fell to 2x10^8 copies g^{-1} after 4 cmbsf and then increased slightly with depth (4x10^8 copies at the bottom of the core). In contrast to DSS and DBB, SEEP SRB-2 16S rDNA copy numbers were low in all samples (maximum of 3x10^8 copies g^{-1} in the bottom of WM12) (Figure 3). SEEP SRB-2 16S rDNA concentrations increased slowly with depth in WMs, reaching 2x10^8 copies g^{-1} in WM14 and fluctuated around 5x10^7 copies g^{-1} throughout EWM14. However no

significant difference of SEEP SRB-2 distributions was detected between habitats (One-way ANOVA, P = 0.088). Quantification of candidate division JS1 16S rRNA gene copies indicated another population dynamic. JS1 16S rDNA copies in the sediment underlying WMs were low but increased with depth until reaching 6.9×10^8 copies g^{-1} for WM12 and 1.2×10^8 copies g^{-1} for WM14. In contrast, in EWM14 sediments, JS1 16S rDNA copy numbers increased rapidly with depth, from 3.3×10^7 copies g^{-1} in the surface sediment layer to 9×10^8 copies g^{-1} at 15 cmbsf (Figure 3) and were higher than potential sulfate-reducers related copy numbers.

FISH visualization of bacterial partners in AOM consortia

FISH observations revealed a high diversity of ANME-2/*Bacteria* consortia in size, shape and organization (Figure 4B). In order to identify bacterial partners involved in the AOM process in Sonora Margin sediments and to observe the distribution of presumed SRB cells inside the aggregates according to the ANME phylogenetic affiliation, FISH experiments were carried out using specific probes targeting sulfate-reducing bacteria (DSS685, DBB660, SEEP2-658, Supplementary Table 2). SEEP SRB-2 *Bacteria,* previously reported as syntrophic AOM involved bacteria (Kleindienst et al., 2012), were observed as single tetrads or in monospecific clusters, but did not show direct physical association with ANME cells (Figure 4A). Nevertheless, SEEP SRB-2 monospecific heaps were occasionally observed in proximity with ANME-1 clusters, probably due to the experimental procedure. SEEP SRB-4 cells were observed as free-living bacteria. ANME-2c *Archaea* were associated with both DSS-hybridized and DBB-hybridized cells and no clear relationship between SRB partner affiliation and morphological appearances of ANME-2c aggregates was observed (Figure 4B). In contrast, ANME-2a formed exclusively intermingled aggregates with DSS-hybridized bacteria (n=124) (Figure 4C). Tight aggregates of ANME-1 were also observed exclusively associated with DSS-hybridized bacterial cells in WM12 deep sediment layers (n=74) (Figure 4D). Clusters of monospecific DSS-hybridized cells (Figure 4E) were observed in EWM14 deep sediment layers when DBB-hybridized cells were only found associated with ANME-2c.

Since only one SRB group per aggregate was detected, DSS and DBB appeared to be exclusive in a given aggregate. Additionally, no other Eubacteria-labeled or unlabeled but DAPI-stained cells were detected in physical proximity of ANME consortia. *Gammaproteobacteria* were observed as large single cells clustered in heaps (Figure 4F) without relationship with ANME.

SEM observations, microanalysis

In order to investigate the physical interaction between ANME and SRB during AOM association, AOM consortia previously localized by FISH (using ANME2c and bacterial probes, Supplementary Table 2) were observed using SEM (Figure 5). Sediments of WM12 harboring higher numbers of ANME-2 and sulfate reducer aggregates were observed. A high amount of sedimented broken diatoms and aggregate-like structures were detected. ANME2c/Bacterial aggregates appeared to be included in a complex and compact matrix, no individual cells or extracellular structures were detected. Microanalysis of these aggregate-like structures revealed a high proportion of organic compounds (55% C, 30% O, 0.39 % K).

Discussion

Overall bacterial diversity at Sonora Margin sediments

Using quantitative PCR analysis, *Bacteria* have been shown to dominate microbial communities in WMs sediments (Vigneron et al., 2013). 16S rRNA gene libraries also demonstrated a higher diversity among *Bacteria* in the sediment, as previously observed in similar cold seep ecosystems (Lloyd et al., 2010; Orcutt et al., 2010), probably corresponding to the wide range of metabolic functions assumed by *Bacteria* in ecosystems (Pace, 1997). Indeed, bacterial populations were diverse in the Sonora Margin sediments, with sequences affiliated to *Deltaproteobacteria,* likely involved in sulfate reduction coupled to the degradation of hydrocarbons or methane in cold seep ecosystems (Dhillon et al., 2003; Knittel et al., 2003; Pereyra et al., 2010) ; *Epsilonproteobacteria* (*Sulfurovum*) and *Gammaproteobacteria* such as *Candidatus Maribeggiatoa*, potentially involved in sulfate

oxidation (Crepeau et al., 2011; Grünke et al., 2011; McKay et al., 2012) and other uncultured lineages, previously detected in oil impacted sediments (Head and Swannell, 1999; Orcutt et al., 2010; Pachiadaki et al., 2010; Pachiadaki et al., 2011). Additionally, *Spirochaetes*, *Firmicutes*, *Acidobacteria, Actinobacteria* and diverse candidate divisions with undetermined metabolic roles in seep environments or potentially involved in organic matter degradation (Rappé and Giovannoni, 2003; Stevens et al., 2005; Pachiadaki et al., 2011) were detected.

Bacterial communities involved in syntrophic AOM

The diversity of bacteria involved in syntrophic AOM with ANME appeared to represent only a third of the total community. Indeed, uncultured lineages of *Gammaproteobacteria,* detected as predominant in gene libraries, were observed as monospecific clusters without any relationship to ANME, suggesting that they were likely not related to the AOM process. The distribution of bacterial lineages, previously suspected to be involved in AOM, was observed throughout the sediment cores in a centimeter scale. Thus, the candidate division JS1, previously detected in deep marine sediments, tidal flat sediments and hydrothermal vents (Webster et al., 2004; Webster et al., 2007; Biddle et al., 2012), and proposed as a possible partner in AOM (Cambon-Bonavita et al., 2009; Harrison et al., 2009; Roalkvam et al., 2011) or in hydrocarbon-degrading and sulfate-reducing consortia (Phelps et al., 1998), was detected in the EWM14 deepest sediment horizons. Specific quantifications of JS1 16S rDNA highlighted increasing 16S rDNA copy numbers with depth, confirming their strictly anoxic ecological niche (Webster et al., 2004). The distribution of candidate division JS1 appeared to mirror the ANME-1 distribution, particularly in EWM14 sediments (r = 0.98, P <0.0001) (Figure 3). However, FISH observations could not validate any bacterial relationship with ANME-1 in EWM14 sediments. These similar distributions of candidate division JS1 and ANME-1 could be due to similar environmental needs/restrictions (methane-rich and reduced environments) rather than to a strict relationship between these microorganisms. The SRB *Deltaproteobacteria* group of SEEP SRB-2, recently observed as

an AOM partner in the Black Sea microbial mats and in the Gulf of Mexico hydrocarbon seeps (Kleindienst et al., 2012) was detected as metabolically active in our samples, and quantified in low abundance throughout sediment cores, without vertical zonation, as previously observed by FISH in the Tommeliten and Gulf of Mexico seeps and in the Guaymas hydrothermal sediments (Kleindienst et al., 2012). However, our FISH observations could not confirm the physical association with ANMEs. Indeed, SEEP SRB-2 were only observed as single tetrads or monospecific clusters, suggesting that, in the Sonora Margin sediments, SEEP SRB-2 could assume another metabolism, as previously proposed (Kleindienst et al., 2012). Likewise, by using previously designed SRB group specific probes (Knittel et al., 2003), the *Deltaproteobacteria* SEEP SRB-4 group was observed as free-living single cells, as previously reported (Orcutt et al., 2010). This would suggest that SEEP SRB-4 groups are more likely involved in hydrocarbon degradation than in AOM process, as previously suggested (Kleindienst et al., 2012). Presence and metabolic activity of such AOM-independent sulfate-reducers could thereby explain the higher sulfate reduction rates compared to the AOM rates, constantly measured in hydrocarbon-rich cold seeps (Bowles et al., 2011). In contrast, our FISH observations showed that both DSS and DBB relatives were strongly associated in consortia with ANMEs, confirming previous studies (Losekann et al., 2007; Pernthaler et al., 2008). While the DSS/ANME-2 associations are ubiquitously detected in cold seep sediments (Knittel and Boetius 2009), the Sonora margin is only the second AOM environment after the Eel River seeps to harbor DBB/ANME-2 consortia (Pernthaler et al. 2008). However, physical associations of other *Bacteria* than *Deltaproteobacteria* within AOM consortia, previously observed by Pernthaler et al., 2008, could not be demonstrated in our samples. In sediments underlying WM14, the proportion of AOM-involved sulfate reducers relative to the total bacterial community, previously estimated by Q-PCR (Vigneron et al., 2013), increased from 2% at the surface layers to 30% at the core bottom. These results are consistent with previous estimates of sulfate-reducer abundance in marine sediments and SMTZ , which ranged from 2% to 35% (Leloup et al., 2007; Leloup et al., 2009). Moreover, high sulfate concentrations throughout WM12

sediments seemed to enhance the relative SRB populations with proportions of up to 70% of the total bacterial community in the core bottom, resulting in an increase in associated ANME abundance. DSS and DBB abundances were comparable in sulfate-riche shallow sediments (0-6 cmbsf) (Figure 3), as previously observed by FISH in Eel River cold seeps (Pernthaler et al., 2008). However, quantification of 16S rDNA gene copy numbers, targeting the DSS and DBB groups, also highlighted significant differences in depth distribution below 6 cmbsf (Figure 3), as previously presumed in a similar environment (Lloyd et al., 2010). This difference in depth distribution might suggest that SRB involved in AOM could have different ecological niches and/or metabolisms despite the apparent same environmental function, as previously suggested (Pernthaler et al., 2008).

DBB *Bacteria*, strictly observed in syntrophic relationship with ANME-2c, were restricted to the sulfate-rich surface sediment layers, except in the microbial mat-sediment interface layer, as previously observed in other underlying mat sediments of cold seep ecosystems (Losekann et al., 2007; Pernthaler et al., 2008; Lloyd et al., 2010). Indeed, in EWM14 (without surficial microbial mat), DBB colonized the upper sediment layers, water-sediment interface included, and a significant correlation was observed between DBB distribution and sulfate pore-water concentrations (r = 0.964, P = 0.0028). This correlation was also observed in WM14 sediments when omitting the surface layer (r = 0.886, P= 0.03). This result, confirming the sulfate-dependant metabolism of DBB bacteria, would also suggest a probable interference between DBB and the microbial mat. Regarding these results, we hypothesize that DBB bacteria could require an organic carbon source, which could also be coveted by *Maribeggiatoa* mats. This carbon source, probably derived from surface inputs, would limit the DBB abundance in the deepest WM12 sediment horizons despite the high sulfate concentrations. Thus, DBB bacteria could support a heterotrophic carbon metabolism, as previously observed in other *Desulfobulbus* family (Sorokin et al., 2012), and participate in the AOM process by reducing the seawater sulfate. Alternatively, the giant filamentous *Maribeggiatoa* from the surface mats, by their movements or activities, could alter the

shallow sediment layers and thereby modify the DBB vertical distribution (Salman et al., 2013). The DBB requirements could partially explain the ANME-2c repartition observed in the Sonora Margin sediments, in particular in EWM14 sediments, where ANME-2c mirror the DBB distributions (r = 0.967, P = 0.0004) (Figure 3). However ANME-2c have also been observed in consortia with DSS bacteria.

The DSS group presented a higher diversity in the gene libraries and at least three of the six previously described SEEP SRB-1 groups (Schreiber et al., 2010) were detected. In EWM14 deep sediments, where no DSS/ANME aggregate was observed, DSS formed monospecific clusters, as previously observed (Omoregie et al., 2008), and gene libraries indicated metabolically active members of the SEEP SRB-1b group, previously suggested as hydrocarbon degraders (Kniemeyer et al., 2007; Schreiber et al., 2010). The DSS 16S rDNA quantifications included the total SEEP SRB-1 (Figure 2), thus the elevated DSS 16S rDNA concentrations in the deepest EWM14 sediment layers could correspond to the SEEP SRB-1b, independent of ANME, as observed by FISH. In contrast, in WMs, a majority of sequences was affiliated to SEEP SRB1a, known to be involved in AOM (Schreiber et al., 2010), and FISH observations highlighted DSS related bacteria in consortia with both ANME-2a,-2c and ANME-1. If sulfate-rich inputs explained a higher DSS abundance throughout WM12 sediments, metabolically active DSS were also detected and quantified in significant proportion (21%) in the deep sulfate-depleted sediments of WM14, which was previously observed in other marine sediments (Leloup et al., 2007; Leloup et al., 2009; Lloyd et al., 2010). Even if we could not exclude that DSS bacteria could require lower sulfate concentrations, previous authors suggested that DSS bacteria might switch to a fermentative process or could benefit from a cryptic sulfate formation (Leloup et al., 2007; Lloyd et al., 2010). Indeed, in marine sediments, sulfide could be re-oxidized to sulfate by abiotic reactions with sea water Fe^{3+} (Yao and Millero, 1996). This sulfate formation would be masked by the DSS sulfate reduction activity at similar rates. Alternatively, DSS, observed within ANME-2c aggregates, could use by disproportionation the intracellular zero-valent

sulfur stored in ANME-2c cells, which forms polysulfides with environmental sulfide, as previously demonstrated in ANME-2c/DSS enrichments (Milucka et al., 2012). Such metabolism, observed by Milucka et al. at low sulfate concentrations (~3mM), would allow the development of these ANME-2c/DSS consortia in sulfate-depleted sediments and thus explain the predominance of DSS and AOM aggregates throughout the WM14 sediment core. Additionally, in contrast to DBB, DSS could use a carbon source available throughout the sediments such as hydrocarbon-derived compounds, as supported by previous DSS enrichments (Dhillon et al., 2003; Kniemeyer et al., 2007), or more likely be lithoautotrophs and assimilate inorganic carbon as recently observed by NanoSIMS analysis of AOM communities (Kellermann et al., 2012; Milucka et al., 2012). Different sulfate requirements, carbon sources and/or environmental interactions for DBB and DSS would account for a distinct distribution of the sulfate-reducing populations and the bacterial partner involved in ANME-2c AOM consortium. The identity of the ANME-2c SRB partners may be dependent on SRB environmental requirements or fluid flow preferences in the sediment. Furthermore, the bacterial partner phylotype did not seem to affect the aggregate morphology (Figure 4). This apparently unspecific and opportunistic association in AOM consortium for ANME-2c could provide a metabolic benefit for ANME-2c, allowing them to colonize a wide range of environmental niches in seep habitats, as compared to ANME-2a (Knittel and Boetius, 2009). This probably also explains the higher ANME-2c abundance estimated by QPCR in the Sonora Margin sediments (Figure 3). Indeed, ANME-2a were observed in mixed and intermingled aggregates exclusively with DSS members, as previously observed (Knittel et al., 2003; Knittel et al., 2005; Schreiber et al., 2010) (Figure 4). This bacterial partner restriction could limit the distribution and abundance of ANME-2a in the Sonora Margin sediments. Likewise, ANME-1 were observed in tight associations only with DSS, as already reported (Orcutt et al., 2005; Maignien et al., 2012). ANME-1 aggregate formation, that we previously suggested to be dependent on a sulfate-concentration threshold (Vigneron et al., 2013), could also be limited by the specificity of their bacterial association. However, the absence of association between ANME-1 and DBB could also be due to antagonist

environmental requirements and therefore different distributions of ANME-1 and DBB. These specificities of partners in AOM consortia as well as the detection of only one SRB group per aggregate could indicate that recognition and control mechanisms exist during the setting up of the relationship between AOM partners. Processes remained unexplained but might potentially involved surface proteins and lipids detection, since different lipid compositions have recently been detected between ANME lineage cell membranes (Rossel et al., 2011). Likewise, the electron, zero-valent sulfur (Milucka et al., 2012), nitrogen (Dekas et al., 2009) and/or potential nutrient transfers between the two microbial partners involved in syntrophic AOM remains enigmatic. Different mechanisms have been proposed such as cell-to-cell contacts (Meyerdierks et al., 2010), use of extracellular proteins such as nanowires or interspecies electron shuttles (Knittel and Boetius, 2009; Stams and Plugge, 2009). SEM visualization of ANME-2c/*Bacteria* aggregates showed that AOM consortia appeared to be included in a complex organic matrix as previously described (Knittel et al., 2005) (Figure 5), probably produced by the consortia themselves. Indeed, the production of extracellular polymers by SRB was previously observed in marine sediments (Zinkevich et al., 1996). As in microbial multi-species biofilms, this organic matrix could protect the microorganisms from environmental stress (oxygen), thus forming a propitious microniche for ANME and SRB,that favors cell-to-cell communications as well as electron or nutrient exchanges (Rickard et al., 2003). This matrix was observed on both large and small aggregates (Figure 5), suggesting a production in the earlier stage in the setting up of the association. This organic boundary could, by the confinement of the first AOM partners, explain the exclusivity of the partnership observed inside aggregates and conserved along the maturation of the aggregate (Nauhaus et al., 2007). Enclosed ANME and SRB would syntrophically grow together inside the matrix, protected from environmental variations or competitive bacterial populations.

Conclusion

With its geochemically diverse habitats, the Sonora margin cold seeps are an appropriate area to explore microbiological processes occurring in surface sediments

percolated by methane and sulfide rich fluids. While ANME populations were shown to dominate archaeal communities, bacteria involved in AOM did not seem to be dominant in Sonora Margin cold seep sediments. A wide diversity of active bacteria was observed. However, only two SRB groups, DSS (probably SEEP SRB1a) and DBB, appear to be exclusively associated with ANME in the Sonora Margin cold seeps. This AOM-involved SRB study highlighted different centimeter scale SRB distributions in cold seep sediments. These SRB appear to exhibit specific habitat preference and spatial configuration with archaeal partners in syntrophic AOM, suggesting that these SRB represent unique ecotypes. Different carbon and sulfate metabolisms (sulfate-reduction, Zero valent sulfur disproportionation) coupled to AOM might occur, depending on SRB phylogeny and probably involving different electron transfer pathways or intermediate and partner recognition mechanisms. Comparative genome analysis of the different ANME partners and NanoSims analysis on enrichments of stable ANME-DBB aggregates might lead to a better understanding of biochemical processes involved in the different AOM consortia.

Experimental Procedures

Sample description

The sediment push cores were sampled at Sonora margin cold seep "Vasconcelos" site during the "BIG" cruise in June 2010. Three different habitats were sampled in the Sonora Margin cold seeps (Supplementary Figure 1). Sediments of White Mat 12 (WM12) and White MAT 14 (WM14) were covered by white bacterial mats, while the water sediment interface of the edge of White Mat14 (EWM14) were colonized by grey polychaetes and gastropods (Vigneron et al., 2013). An autonomous temperature sensor (T-Rov, NKE Electronics, France) indicated *in situ* temperatures of 3°C from the surface water to 50 cmbsf in each habitat before sampling. Immediately after recovery, sediment cores were transferred into a cold room, then aseptically sub-sampled in 2 cm thick layers and conditioned for molecular and FISH experiments. The sampling strategy and experimental procedures used in this

study were detailed in a previous work based on an archaeal survey (Vigneron et al., 2013). Detailed geochemical measurements and ANME concentrations are provided in Figure 3.

Sediment RNA extractions, cDNA clone libraries and sequencing.

16S rRNA amplification was used as a proxy for the detection of active microbial populations (Lloyd et al., 2010). RNA was extracted using the Zhou protocol (Zhou et al., 1996) with modifications (Lazar et al., 2010) and purified using Nucleospin® RNA II kit (Macherey Nagel, Düren, Germany). Absence of residual DNA contamination was verified by PCR. Reverse transcription PCR of 16S rRNA were carried out by a two-step protocol with a preliminary reverse transcription step using Quanta qScript® kit (Quanta Bioscience, Gaithersburg, MD, USA). PCR reactions contained 10 ng of reverse transcribed RNA template,1 X PCR Buffer, 2nM $MgCl_2$, 0.2 mM of each dNTP, 0.4 mM of each primer (E338f 5'- ACT CCT ACG GGA GGC AGC-3' and U1407r 5'-GAC GGG CGG TGW GTR CAA-3') and 0.6 U *GoTaq* DNA polymerase (Promega BioSciences, San Luis Obispo CA, USA). Amplifications were carried out using the GeneAmp PCR 9700 System (Applied Biosystems, Foster City, CA, USA) as follows: denaturation step at 94°C for 1 min, annealing for 1 min 30 s at 54°C and extension step for 2 min at 72°C for 30 cycles. For gene library construction, the 16S rRNA were reverse transcribed, amplified in triplicate and pooled before gel purification. Purified amplification products were cloned into TOPO® XL PCR Cloning Kit, and transformed into *Escherichia coli* TOP10 cells (Invitrogen, Carlsbad, CA, USA) according to the manufacturer's recommendations. 16S rRNA gene sequences were determined on an ABI3730xl – genetic Analyzer using M13 universal primers (GATC Biotech, Germany). Sequences were analyzed using the NCBI BLASTn search program within GenBank (Altschul et al., 1990). Sequences were aligned with closest representative sequences from GenBank using MAFFT 6.903 (Katoh et al., 2005) and checked manually for chimera. Phylogenetic trees were estimated with maximum likelihood methods, using MPI-parallelized RAxML 7.2.8. (Stamatakis, 2006) on the CIPRES Science Gateway (Miller et al., 2011). GTRCAT approximation of models was used for ML bootstrapping (1000). Simpson indexes

were calculated using DOTUR as previously detailed (Guri et al., 2012). Sequences from cDNA libraries affiliated to the *Deltaproteobacteria* were deposited in the EMBL database under accession numbers: HE972157-HE972208 and other *Bacteria* under HF545525-HF545595.

Quantitative real-time PCR

Real-time PCR amplifications were performed in triplicate using Perfecta® SYBR® Green SuperMix ROX (Quanta Bioscience) according to the manufacturer's recommendations. Amplifications followed a two step PCR (40 cycles) with 15 s denaturation (95°C) and 1 min annealing/elongation step at 60°C. Primer concentrations were optimized, as recommended by the manufacturer, to minimize the formation of secondary structure and to maximize the efficiency of the reaction. New primer sets, specific for SRB groups and candidate division JS1, were designed using the ARB package (Ludwig et al., 2004) and web-based application Primaclade (Gadberry et al., 2005) and are listed in Supplementary Table 1. Primers were checked for specificity by using *Oligocheck* software and tested by PCR on various environmental clones from the Sonora Margin sediments. Triplicate standard curves were obtained with ten-fold serial dilutions of plasmids containing environmental 16S rRNA sequences relative to DSS, DBB, SEEP SRB-2 or JS1 and ranged from 10^4 to 10^8 copies/µL of 16S rDNA. The R^2 of standard curves obtained by real time PCR were up to 0.997 and efficiency of the reaction up to 98%. The primer set specificity was confirmed by control sequencing of amplification products. Samples were diluted to a concentration for which no inhibitory effect was observed. Correlation factors and statistical tests on the microbial distribution were achieved using Graph Pad Prism Software.

Fluorescence In Situ Hybridizations (FISH)

Immediately after the core recovery, two grams of sediment collected from each layer were fixed in PBS (1X)/formaldehyde (3% final) at 4°C for 4 hours then washed twice with PBS(1X) and stored in PBS(2X)/Ethanol (1:1, vol/vol) buffer at -20°C. Twenty microlitres of a

100 fold dilution of the sample were immobilized on 0.22 µm GTTP polycarbonate filters (Merck Milipore, Darmstadt, Germany) for FISH observations. For filters observed by SEM after FISH, fixed sediments were sonicated (40 fold 1 sec, 40% intensity, Vibra Cell, Biolock Scientific, France) before immobilization on fine-tipped pen squared filters. Hybridization was carried out for 3 hours at 46°C in formamide buffer with labeled probes (Supplementary Table 2). After 20 min in washing buffer at 48°C, filters were fixed on slides and covered with an antifade/DAPI solution (SlowFade® Gold, Invitrogen). As cross hybridization between DSS and SEEP SRB-2 probes was recently observed (Kleindienst et al., 2012), detection of AOM-involved SRB were monitored combining the three SRB probes with 50% formamide and no co-localized signal was detected. In order to conclude on the aggregate morphologies and partnership specificities, two replicate filters (each harboring over 100 aggregates) were fully explored for each sediment layer previously analyzed by gene libraries. Observations and imaging were performed using an epifluorescence Axio Imager Z2 microscope equipped with the Apotome® system and the COLIBRI® technology (Zeiss, Jena, Germany). ANME/*Bacteria* aggregate location was noted in order to be observed by SEM.

Scanning Electron Microscopy (SEM)

Immediately after FISH observations, filters were completely dried at room temperature and then directly metalized with gold and palladium (60/40) using a high resolution Sputter Coater (Quorum Technologies, Guelph, Canada). SEM observations and imaging were performed using a FEI Quanta 200 microscope (FEI, Oregon, USA) and micro analyzes performed with EDX microelectrode (Oxford instruments, Abingdon, UK).

Acknowledgements

We are indebted to the crews of the research vessel *L'Atalante* and the submersible *Nautile* of the cruise "BIG" and the scientific team for their contribution in sampling on board. This

cruise and work was funded by IFREMER (France) and has benefited from a work permit in Mexican waters (DAPA/2/281009/3803, October 28th, 2009).

References

Altschul, S.F., Gish, W., Miller, W., Myers, E.W., and Lipman, D.J. (1990) Basic local alignment search tool. *J Mol Biol* **215**: 403-410.

Beal, E.J., House, C.H., and Orphan, V.J. (2009) Manganese- and iron-dependent marine methane oxidation. *Science* **325**: 184-187.

Biddle, J.F., Cardman, Z., Mendlovitz, H., Albert, D.B., Lloyd, K.G., Boetius, A., and Teske, A. (2012) Anaerobic oxidation of methane at different temperature regimes in Guaymas Basin hydrothermal sediments. *Isme Journal* **6**: 1018-1031.

Boetius, A., Ravenschlag, K., Schubert, C.J., Rickert, D., Widdel, F., Gieseke, A. et al. (2000) A marine microbial consortium apparently mediating anaerobic oxidation of methane. *Nature* **407**: 623-626.

Bowles, M.W., Samarkin, V.A., Bowles, K.M., and Joye, S.B. (2011) Weak coupling between sulfate reduction and the anaerobic oxidation of methane in methane-rich seafloor sediments during ex situ incubation. *Geochimica Et Cosmochimica Acta* **75**: 500-519.

Cambon-Bonavita, M.A., Nadalig, T., Roussel, E., Delage, E., Duperron, S., Caprais, J.C. et al. (2009) Diversity and distribution of methane-oxidizing microbial communities associated with different faunal assemblages in a giant pockmark of the Gabon continental margin. *Deep-Sea Research Part Ii-Topical Studies in Oceanography* **56**: 2248-2258.

Crepeau, V., Bonavita, M.A.C., Lesongeur, F., Randrianalivelo, H., Sarradin, P.M., Sarrazin, J., and Godfroy, A. (2011) Diversity and function in microbial mats from the Lucky Strike hydrothermal vent field. *FEMS Microbiol Ecol* **76**: 524-540.

Dekas, A.E., Poretsky, R.S., and Orphan, V.J. (2009) Deep-sea archaea fix and share nitrogen in methane-consuming microbial consortia. *Science* **326**: 422-426.

Dhillon, A., Teske, A., Dillon, J., Stahl, D.A., and Sogin, M.L. (2003) Molecular characterization of sulfate-reducing bacteria in the Guaymas Basin. *Appl Environ Microbiol* **69**: 2765-2772.

Ettwig, K.F., Butler, M.K., Le Paslier, D., Pelletier, E., Mangenot, S., Kuypers, M.M.M. et al. (2010) Nitrite-driven anaerobic methane oxidation by oxygenic bacteria. *Nature* **464**: 543-+.

Gadberry, M.D., Malcomber, S.T., Doust, A.N., and Kellogg, E.A. (2005) Primaclade--a flexible tool to find conserved PCR primers across multiple species. *Bioinformatics* **21**: 1263-1264.

Grünke, S., Felden, J., Lichtschlag, A., Girnth, A.C., De Beer, D., WenzhÖFer, F., and Boetius, A. (2011) Niche differentiation among mat-forming, sulfide-oxidizing bacteria at cold seeps of the Nile Deep Sea Fan (Eastern Mediterranean Sea). *Geobiology* **9**: 330-348.

Guri, M., Durand, L., Cueff-Gauchard, V., Zbinden, M., Crassous, P., Shillito, B., and Cambon-Bonavita, M.A. (2012) Acquisition of epibiotic bacteria along the life cycle of the hydrothermal shrimp Rimicaris exoculata. *Isme Journal* **6**: 597-609.

Harrison, B.K., Zhang, H., Berelson, W., and Orphan, V.J. (2009) Variations in archaeal and bacterial diversity associated with the sulfate-methane transition zone in continental margin sediments (Santa Barbara Basin, California). *Appl Environ Microbiol* **75**: 1487-1499.

Head, I.M., and Swannell, R.P.J. (1999) Bioremediation of petroleum hydrocarbon contaminants in marine habitats. *Current Opinion in Biotechnology* **10**: 234-239.

Holler, T., Widdel, F., Knittel, K., Amann, R., Kellermann, M.Y., Hinrichs, K.U. et al. (2011) Thermophilic anaerobic oxidation of methane by marine microbial consortia. *ISME J* **5**: 1946-1956.

Inagaki, F., Tsunogai, U., Suzuki, M., Kosaka, A., Machiyama, H., Takai, K. et al. (2004) Characterization of C1-metabolizing prokaryotic communities in methane seep habitats at the Kuroshima Knoll, southern Ryukyu Arc, by analyzing pmoA, mmoX, mxaF, mcrA, and 16S rRNA genes. *Appl Environ Microbiol* **70**: 7445-7455.

Jorgensen, B.B., and Boetius, A. (2007) Feast and famine--microbial life in the deep-sea bed. *Nat Rev Microbiol* **5**: 770-781.

Katoh, K., Kuma, K., Toh, H., and Miyata, T. (2005) MAFFT version 5: improvement in accuracy of multiple sequence alignment. *Nucleic Acids Research* **33**: 511-518.

Kellermann, M.Y., Wegener, G., Elvert, M., Yoshinaga, M.Y., Lin, Y.-S., Holler, T. et al. (2012) Autotrophy as a predominant mode of carbon fixation in anaerobic methane-oxidizing microbial communities. *Proceedings of the National Academy of Sciences* **109**: 19321-19326.

Kleindienst, S., Ramette, A., Amann, R., and Knittel, K. (2012) Distribution and in situ abundance of sulfate-reducing bacteria in diverse marine hydrocarbon seep sediments. *Environ Microbiol*: no-no.

Kniemeyer, O., Musat, F., Sievert, S.M., Knittel, K., Wilkes, H., Blumenberg, M. et al. (2007) Anaerobic oxidation of short-chain hydrocarbons by marine sulphate-reducing bacteria. *Nature* **449**: 898-U810.

Knittel, K., and Boetius, A. (2009) Anaerobic Oxidation of Methane: Progress with an Unknown Process. *Annual Review of Microbiology* **63**: 311-334.

Knittel, K., Losekann, T., Boetius, A., Kort, R., and Amann, R. (2005) Diversity and distribution of methanotrophic archaea at cold seeps. *Appl Environ Microbiol* **71**: 467-479.

Knittel, K., Boetius, A., Lemke, A., Eilers, H., Lochte, K., Pfannkuche, O. et al. (2003) Activity, distribution, and diversity of sulfate reducers and other bacteria in sediments above gas hydrate (Cascadia margin, Oregon). *Geomicrobiology Journal* **20**: 269-294.

Lazar, C.S., Dinasquet, J., Pignet, P., Prieur, D., and Toffin, L. (2010) Active archaeal communities at cold seep sediments populated by Siboglinidae tubeworms from the Storegga Slide. *Microb Ecol* **60**: 516-527.

Leloup, J., Loy, A., Knab, N.J., Borowski, C., Wagner, M., and Jorgensen, B.B. (2007) Diversity and abundance of sulfate-reducing microorganisms in the sulfate and methane zones of a marine sediment, Black Sea. *Environ Microbiol* **9**: 131-142.

Leloup, J., Fossing, H., Kohls, K., Holmkvist, L., Borowski, C., and Jorgensen, B.B. (2009) Sulfate-reducing bacteria in marine sediment (Aarhus Bay, Denmark): abundance and diversity related to geochemical zonation. *Environmental Microbiology* **11**: 1278-1291.

Lloyd, K.G., Albert, D.B., Biddle, J.F., Chanton, J.P., Pizarro, O., and Teske, A. (2010) Spatial structure and activity of sedimentary microbial communities underlying a Beggiatoa spp. mat in a Gulf of Mexico hydrocarbon seep. *PLoS One* **5**: e8738.

Losekann, T., Knittel, K., Nadalig, T., Fuchs, B., Niemann, H., Boetius, A., and Amann, R. (2007) Diversity and abundance of aerobic and anaerobic methane oxidizers at the Haakon Mosby Mud Volcano, Barents Sea. *Appl Environ Microbiol* **73**: 3348-3362.

Ludwig, W., Strunk, O., Westram, R., Richter, L., Meier, H., Yadhukumar et al. (2004) ARB: a software environment for sequence data. *Nucleic Acids Res* **32**: 1363-1371.

Maignien, L., Parkes, R.J., Cragg, B., Niemann, H., Knittel, K., Coulon, S. et al. (2012) Anaerobic oxidation of methane in hypersaline cold seep sediments. *FEMS Microbiol Ecol*: n/a-n/a.

McKay, L.J., MacGregor, B.J., Biddle, J.F., Albert, D.B., Mendlovitz, H.P., Hoer, D.R. et al. (2012) Spatial heterogeneity and underlying geochemistry of phylogenetically diverse orange and white Beggiatoa mats in Guaymas Basin hydrothermal sediments. *Deep Sea Research Part I: Oceanographic Research Papers* **67**: 21-31.

Meyerdierks, A., Kube, M., Kostadinov, I., Teeling, H., Glockner, F.O., Reinhardt, R., and Amann, R. (2010) Metagenome and mRNA expression analyses of anaerobic methanotrophic archaea of the ANME-1 group. *Environ Microbiol* **12**: 422-439.

Miller, M.A., Pfeiffer, W., and Schwartz, T. (2011) The CIPRES science gateway: a community resource for phylogenetic analyses. In *Proceedings of the 2011 TeraGrid Conference: Extreme Digital Discovery*. Salt Lake City, Utah: ACM, pp. 1-8.

Milucka, J., Ferdelman, T.G., Polerecky, L., Franzke, D., Wegener, G., Schmid, M. et al. (2012) Zero-valent sulphur is a key intermediate in marine methane oxidation. *Nature* **491**: 541-+.

Nauhaus, K., Albrecht, M., Elvert, M., Boetius, A., and Widdel, F. (2007) In vitro cell growth of marine archaeal-bacterial consortia during anaerobic oxidation of methane with sulfate. *Environ Microbiol* **9**: 187-196.

Niemann, H., Losekann, T., de Beer, D., Elvert, M., Nadalig, T., Knittel, K. et al. (2006) Novel microbial communities of the Haakon Mosby mud volcano and their role as a methane sink. *Nature* **443**: 854-858.

Omoregie, E.O., Mastalerz, V., de Lange, G., Straub, K.L., Kappler, A., Roy, H. et al. (2008) Biogeochemistry and community composition of iron- and sulfur-precipitating microbial mats at the Chefren mud volcano (Nile Deep Sea Fan, Eastern Mediterranean). *Appl Environ Microbiol* **74**: 3198-3215.

Orcutt, B., Boetius, A., Elvert, M., Samarkin, V., and Joye, S.B. (2005) Molecular biogeochemistry of sulfate reduction, methanogenesis and the anaerobic oxidation of methane at Gulf of Mexico cold seeps. *Geochimica Et Cosmochimica Acta* **69**: 4267-4281.

Orcutt, B.N., Joye, S.B., Kleindienst, S., Knittel, K., Ramette, A., Reitz, A. et al. (2010) Impact of natural oil and higher hydrocarbons on microbial diversity, distribution, and activity in Gulf of Mexico cold-seep sediments. *Deep Sea Research Part II: Topical Studies in Oceanography* **57**: 2008-2021.

Orphan, V.J., House, C.H., Hinrichs, K.U., McKeegan, K.D., and DeLong, E.F. (2002) Multiple archaeal groups mediate methane oxidation in anoxic cold seep sediments. *Proceedings of the National Academy of Sciences of the United States of America* **99**: 7663-7668.

Pace, N.R. (1997) A Molecular View of Microbial Diversity and the Biosphere. *Science* **276**: 734-740.

Pachiadaki, M.G., Lykousis, V., Stefanou, E.G., and Kormas, K.A. (2010) Prokaryotic community structure and diversity in the sediments of an active submarine mud volcano (Kazan mud volcano, East Mediterranean Sea). *FEMS Microbiol Ecol* **72**: 429-444.

Pachiadaki, M.G., Kallionaki, A., Dahlmann, A., De Lange, G.J., and Kormas, K.A. (2011) Diversity and spatial distribution of prokaryotic communities along a sediment vertical profile of a deep-sea mud volcano. *Microb Ecol* **62**: 655-668.

Paull, C.K., Ussler, W., Peltzer, E.T., Brewer, P.G., Keaten, R., Mitts, P.J. et al. (2007) Authigenic carbon entombed in methane-soaked sediments from the northeastern transform margin of the Guaymas Basin, Gulf of California. *Deep-Sea Research Part Ii-Topical Studies in Oceanography* **54**: 1240-1267.

Pereyra, L.P., Hiibel, S.R., Riquelme, M.V.P., Reardon, K.F., and Pruden, A. (2010) Detection and Quantification of Functional Genes of Cellulose-Degrading, Fermentative, and Sulfate-Reducing Bacteria and Methanogenic Archaea. *Appl Environ Microbiol* **76**: 2192-2202.

Pernthaler, A., Dekas, A.E., Brown, C.T., Goffredi, S.K., Embaye, T., and Orphan, V.J. (2008) Diverse syntrophic partnerships from deep-sea methane vents revealed by direct cell capture and metagenomics. *Proc Natl Acad Sci U S A* **105**: 7052-7057.

Phelps, C.D., Kerkhof, L.J., and Young, L.Y. (1998) Molecular characterization of a sulfate-reducing consortium which mineralizes benzene. *FEMS Microbiol Ecol* **27**: 269-279.

Raghoebarsing, A.A., Pol, A., van de Pas-Schoonen, K.T., Smolders, A.J.P., Ettwig, K.F., Rijpstra, W.I.C. et al. (2006) A microbial consortium couples anaerobic methane oxidation to denitrification. *Nature* **440**: 918-921.

Rappé, M.S., and Giovannoni, S.J. (2003) THE UNCULTURED MICROBIAL MAJORITY. *Annual Review of Microbiology* **57**: 369-394.

Rickard, A.H., Gilbert, P., High, N.J., Kolenbrander, P.E., and Handley, P.S. (2003) Bacterial coaggregation: an integral process in the development of multi-species biofilms. *Trends Microbiol* **11**: 94-100.

Roalkvam, I., Jorgensen, S.L., Chen, Y.F., Stokke, R., Dahle, H., Hocking, W.P. et al. (2011) New insight into stratification of anaerobic methanotrophs in cold seep sediments. *FEMS Microbiol Ecol* **78**: 233-243.

Rossel, P.E., Elvert, M., Ramette, A., Boetius, A., and Hinrichs, K.-U. (2011) Factors controlling the distribution of anaerobic methanotrophic communities in marine environments: Evidence from intact polar membrane lipids. *Geochimica Et Cosmochimica Acta* **75**: 164-184.

Salman, V., Bailey, J.V., and Teske, A. (2013) Phylogenetic and morphologic complexity of giant sulphur bacteria. *Antonie Van Leeuwenhoek* **104**: 169-186.

Schreiber, L., Holler, T., Knittel, K., Meyerdierks, A., and Amann, R. (2010) Identification of the dominant sulfate-reducing bacterial partner of anaerobic methanotrophs of the ANME-2 clade. *Environ Microbiol* **12**: 2327-2340.
Schubert, C.J., Vazquez, F., Losekann-Behrens, T., Knittel, K., Tonolla, M., and Boetius, A. (2011) Evidence for anaerobic oxidation of methane in sediments of a freshwater system (Lago di Cadagno). *FEMS Microbiol Ecol* **76**: 26-38.
Simoneit, B.R.T., Lonsdale, P.F., Edmond, J.M., and Shanks, W.C. (1990) Deep-Water Hydrocarbon Seeps in Guaymas Basin, Gulf of California. *Applied Geochemistry* **5**: 41-49.
Sorokin, D.Y., Tourova, T.P., Panteleeva, A.N., and Muyzer, G. (2012) Desulfonatronobacter acidivorans gen. nov., sp. nov. and Desulfobulbus alkaliphilus sp. nov., haloalkaliphilic heterotrophic sulfate-reducing bacteria from soda lakes. *International Journal of Systematic and Evolutionary Microbiology* **62**: 2107-2113.
Stamatakis, A. (2006) RAxML-VI-HPC: maximum likelihood-based phylogenetic analyses with thousands of taxa and mixed models. *Bioinformatics* **22**: 2688-2690.
Stams, A.J.M., and Plugge, C.M. (2009) Electron transfer in syntrophic communities of anaerobic bacteria and archaea. *Nature Reviews Microbiology* **7**: 568-577.
Stevens, H., Stübner, M., Simon, M., and Brinkhoff, T. (2005) Phylogeny of Proteobacteria and Bacteroidetes from oxic habitats of a tidal flat ecosystem. *FEMS Microbiol Ecol* **54**: 351-365.
Vigneron, A., Cruaud, P., Pignet, P., Caprais, J.-C., Cambon-Bonavita, M.-A., Godfroy, A., and Toffin, L. (2013) Archaeal and anaerobic methane oxidizer communities in the Sonora Margin cold seeps, Guaymas Basin (Gulf of California). *ISME J*.
Webster, G., Parkes, R.J., Fry, J.C., and Weightman, A.J. (2004) Widespread occurrence of a novel division of bacteria identified by 16S rRNA gene sequences originally found in deep marine Sediments. *Appl Environ Microbiol* **70**: 5708-5713.
Webster, G., Yarram, L., Freese, E., Koster, J., Sass, H., Parkes, R.J., and Weightman, A.J. (2007) Distribution of candidate division JS1 and other Bacteria in tidal sediments of the German Wadden Sea using targeted 16S rRNA gene PCR-DGGE. *FEMS Microbiol Ecol* **62**: 78-89.
Yao, W., and Millero, F.J. (1996) Oxidation of hydrogen sulfide by hydrous Fe(III) oxides in seawater. *Marine Chemistry* **52**: 1-16.
Zhou, J., Bruns, M.A., and Tiedje, J.M. (1996) DNA recovery from soils of diverse composition. *Appl Environ Microbiol* **62**: 316-322.
Zinkevich, V., Bogdarina, I., Kang, H., Hill, M.A.W., Tapper, R., and Beech, I.B. (1996) Characterisation of exopolymers produced by different isolates of marine sulphate-reducing bacteria. *International Biodeterioration & Biodegradation* **37**: 163-172.

Table and Figure legends

Figure 1: Phylogenetic affiliations of bacterial 16S cDNA sequences for cold seep sediments of the Sonora Margin from Top (0 to 4 cmbsf), Middle (4 to 6 cmbsf) and Bottom (8 to 12 cmbsf). Shades of red, green, and blue denote putative *Proteobacteria* (Epsilon-, Delta- and Gamma- respectively). A,B and C correspond to the three selected habitats : white MAT12, White MAT14 and Edge of White MAT14.

Figure 2: Maximum Likelihood phylogenetic tree of the bacterial *Deltaproteobacteria* 16S cDNA sequences in sediments of the Sonora Margin cold seeps performed using RAxML

7.2.8 and GTRCAT model approximation with 1000 replicates. Only bootstrap values up to 70 % are shown. Sequences amplified from sections 0 to 4 cmbsf are labeled "Top", sequences from 4 to 6 cmbsf are "Middle" and sequences from 8 cmbsf to end are tagged "Bottom". Only one representative sequence (>97% identical) is shown. Number in brackets shown the number of clones analyzed from RNA clone libraries. Dotted lines and dashes indicate sequences matching with corresponding Q-PCR primers and FISH probes, respectively. White MAT12, WM12; White MAT14, WM14; EWM14, Edge of White MAT14.

Figure 3: I Geochemical description of the three selected habitats **A)** White MAT12 (WM12), **B)** White MAT14 (WM14) and **C)** Edge White MAT14 (EWM14). Dissolved methane (cross), sulfate (open square) and sulfide (black square) concentrations in porewaters. **II** DNA copy numbers of the 16S rDNA gene per gram of sediment for ANME groups previously observed on the same samples in the Sonora Margin sediments (Vigneron et al. 2013). **III** DNA copy numbers of the 16S rDNA gene per gram of sediment for bacterial groups *Desulfosarcina*/*Desulfoccocus*, *Desulfobulbus*, SEEP SRB2 and candidate division JS1 in function of depth (0 to 15 cmbsf) in cold seep sediments of the Sonora Margin. Differences between DSS and DBB abundances were tested with t-test and labeled with ***P<0.0001, **P<0.001 and *P<0.01. **IV** Proportion of sulfate reducing bacteria to total bacterial community previously estimated by Q-PCR

Figure 4: Individual cells and cell aggregates of ANMEs and bacterial partners visualized with fluorescent-labeled oligonucleotide probes. Each presented aggregate was taken from different pictures. A_1 and A_2) Monophyletic aggregate and single tetrad of SEEP SRB2 labeled with SEEP2-658 (Orange). B) Aggregates of ANME-2c (ANME2c-622 Yellow) and *DSS* cells (B1 and B3) or *DBB* cells (B2). C) Mixed aggregate of ANME-2a (ANME2a-647/*DSS* (DSS-658 green). D) Tight aggregates of ANME-1 (ANME-1-350 -Yellow) and *DSS* (DSS-658 Green). E) Homogeneous aggregate of *DSS* cells labeled with DSS-658 probe (Green). F) Monospecific clusters of *Gammaproteobacteria* cells labeled with GAM42a probe (Blue). Scale is 10 µm. Pictures A B and F were from WM14 middle sediment layer, picture C

from WM12 middle sediment layer, picture D from the bottom sediment layer of WM12 and picture E from the deepest sediment layer of EWM14.

Figure 5: FISH (A_1 and B_1) and SEM (A_2 and B_2) observations of ANME-2c/*Bacteria* aggregates on WM12 bottom sediment layers.

Supplementary Material

Supplementary Figure 1: Schematic view of sampling sites around markers BIG18 (N 27°35.5781; W 111°28.9848) with *Nautile* dives areas (PL), relative position of push cores (CT, Diameter 5 cm, length 30 cm) and their geochemical measurements (CH_4 for methane concentrations, SO_4 for sulfate and H_2S for sulfide) and microbiological analysis (M). Scale is 1 meter. Modified from Vigneron et al., 2013.

Supplementary Figure 2: Maximum Likelihood phylogenetic tree of the bacterial 16S cDNA sequences in the Guaymas Basin cold seep sediments, performed using RAxML 7.2.8 and GTRCAT model approximation with 1000 replicates. Only bootstrap values above 70 % are shown. Sequences amplified from sections 0 to 4 cmbsf are labeled "Top", sequences from 4 to 6 cmbsf are "Middle" and sequences from 8 cmbsf to the end of the core are tagged "Bottom". Only one representative sequence is shown. Number in brackets indicate the number of similar clones (above 97% similarity). White MAT12, WM12; White MAT14, WM14; EWM14, Edge of White MAT14.

Supplementary Table 1: PCR primers used for real-time PCR of 16S rDNA genes.

Supplementary Table 2: Oligonucleotide probes used for fluorescence *in situ* hybridization.

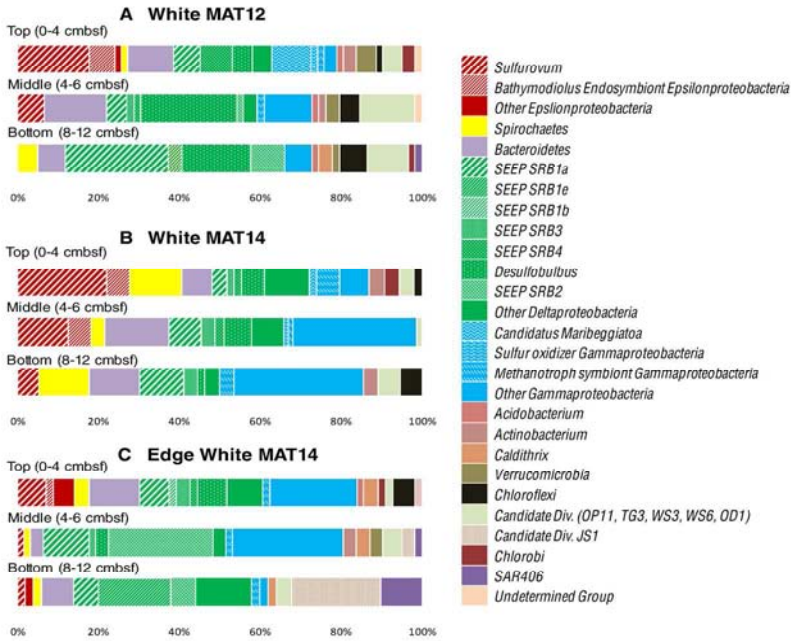

Phylogenetic affiliations of bacterial 16S cDNA sequences for cold seep sediments of the Sonora Margin from Top (0 to 4 cmbsf), Middle (4 to 6 cmbsf) and Bottom (8 to 12 cmbsf). Shades of red, green, and blue denote putative *Proteobacteria* (Epsilon-, Delta- and Gamma- respectively). A,B and C correspond to the three selected habitats : white MAT12, White MAT14 and Edge of White MAT14.
648x458mm (72 x 72 DPI)

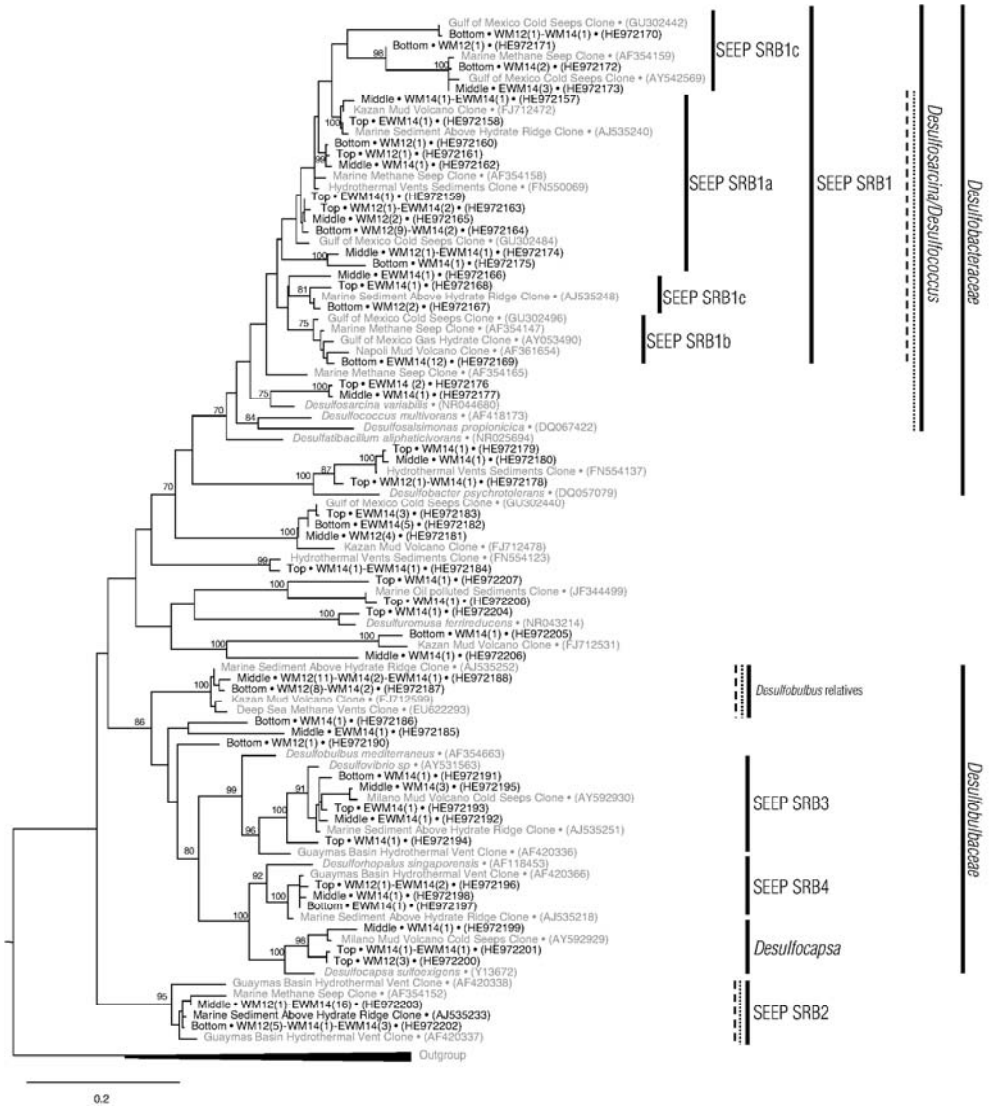

Maximum Likelihood phylogenetic tree of the bacterial *Deltaproteobacteria* 16S cDNA sequences in sediments of the Sonora Margin cold seeps performed using RAxML 7.2.8 and GTRCAT model approximation with 1000 replicates. Only bootstrap values up to 70 % are shown. The scale bar indicates five substitutions per 100 nucleotides. Sequences amplified from sections 0 to 4 cmbsf are labeled "Top", sequences from 4 to 6 cmbsf are "Middle" and sequences from 8 cmbsf to end are tagged "Bottom". Only one representative sequence (>97% identical) is shown. Number in brackets shown the number of clones analyzed from RNA clone libraries. Dotted lines and dashes indicate sequences matching with corresponding Q-PCR primers and FISH probes, respectively. White MAT12, WM12; White MAT14, WM14; EWM14, Edge of White MAT14. 188x208mm (300 x 300 DPI)

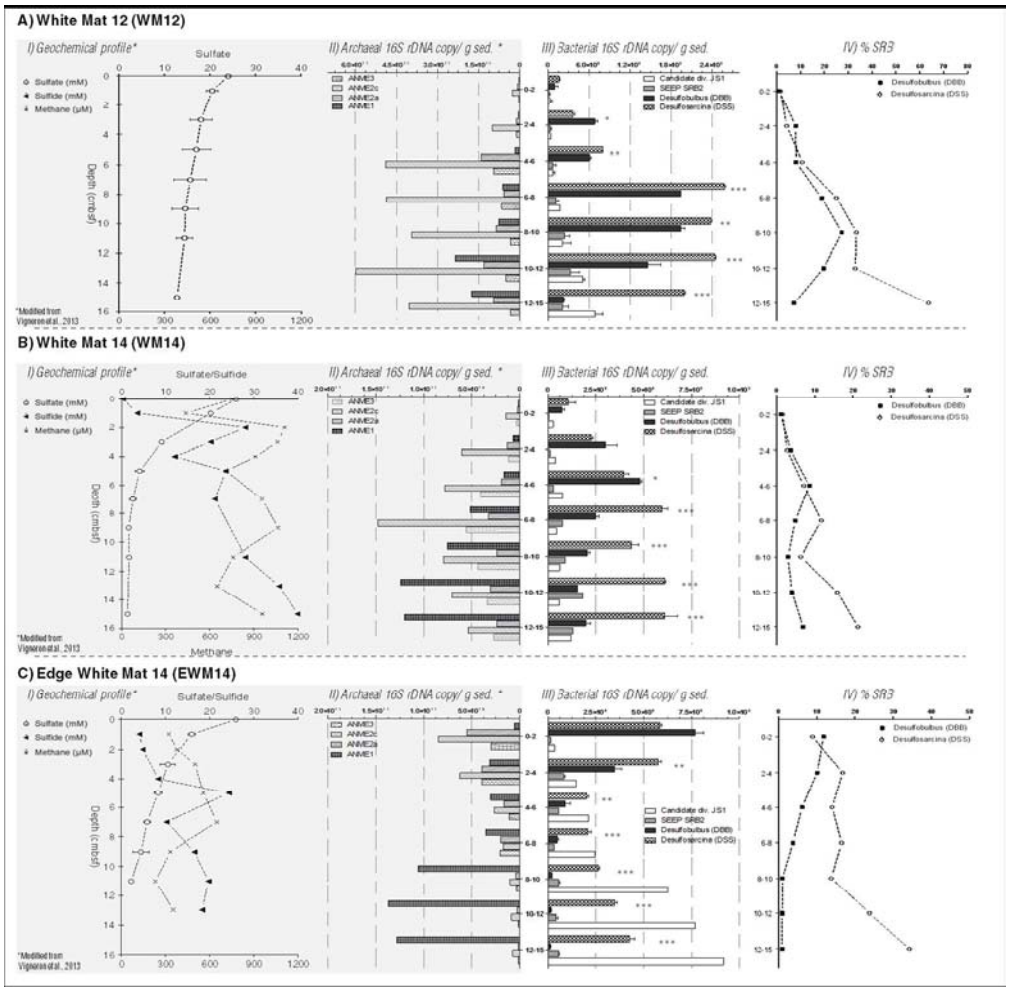

I Geochemical description of the three selected habitats A) White MAT12 (WM12), B) White MAT14 (WM14) and C) Edge White MAT14 (EWM14). Dissolved methane (cross), sulfate (open square) and sulfide (black square) concentrations in porewaters. II DNA copy numbers of the 16S rDNA gene per gram of sediment for ANME groups previously observed on the same samples in the Sonora Margin sediments (Vigneron et al. 2013). III DNA copy numbers of the 16S rDNA gene per gram of sediment for bacterial groups *Desulfosarcina/Desulfoccocus, Desulfobulbus*, SEEP SRB2 and candidate division JS1 in function of depth (0 to 15 cmbsf) in cold seep sediments of the Sonora Margin. Differences between DSS and DBB abundances were tested with t-test and labeled with ***P<0.0001, **P<0.001 and *P<0.01. IV Proportion of sulfate reducing bacteria to total bacterial community previously estimated by Q-PCR
260x255mm (150 x 150 DPI)

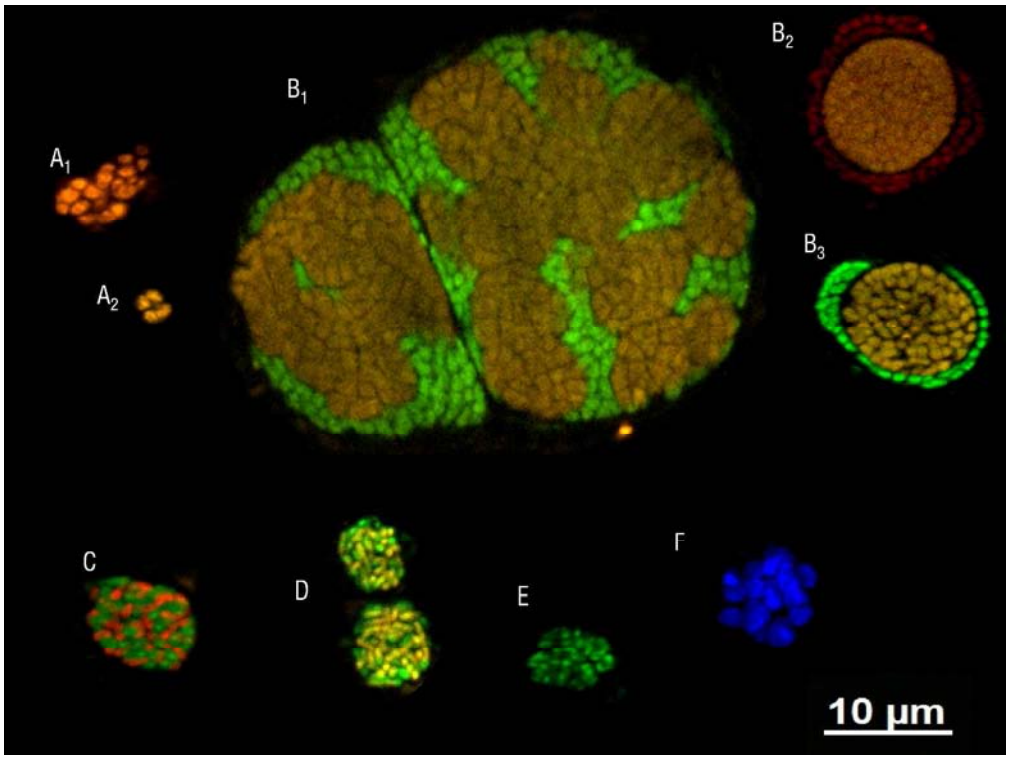

Individual cells and cell aggregates of ANMEs and bacterial partners visualized with fluorescent-labeled oligonucleotide probes. Each presented aggregate was taken from different pictures. A1 and A2) Monophyletic aggregate and single tetrad of SEEP SRB2 labeled with SEEP2-658 (Orange). B) Aggregates of ANME-2c (ANME2c-622 Yellow) and DSS cells (B1 and B3) or DBB cells (B2). C) Mixed aggregate of ANME-2a (ANME2a-647/DSS (DSS-658 green). D) Tight aggregates of ANME-1 (ANME-1-350 -Yellow) and DSS (DSS-658 Green). E) Homogeneous aggregate of DSS cells labeled with DSS-658 probe (Green). F) Monospecific clusters of *Gammaproteobacteria* cells labeled with GAM42a probe (Blue). Scale is 10 µm. Pictures A B and F were from WM14 middle sediment layer, picture C from WM12 middle sediment layer, picture D from the bottom sediment layer of WM12 and picture E from the deepest sediment layer of EWM14.
253x189mm (300 x 300 DPI)

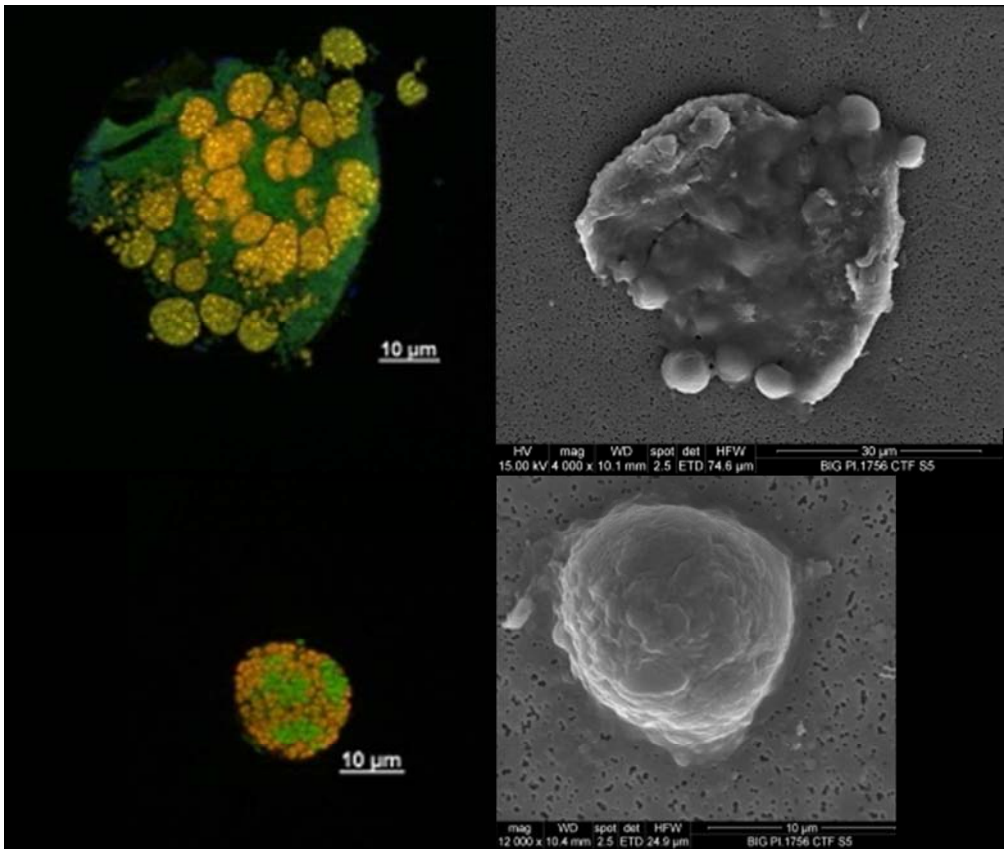

FISH (A1 and B1) and SEM (A2 and B2) observations of ANME-2c/*Bacteria* aggregates on WM12 bottom sediment layers.
284x240mm (150 x 150 DPI)

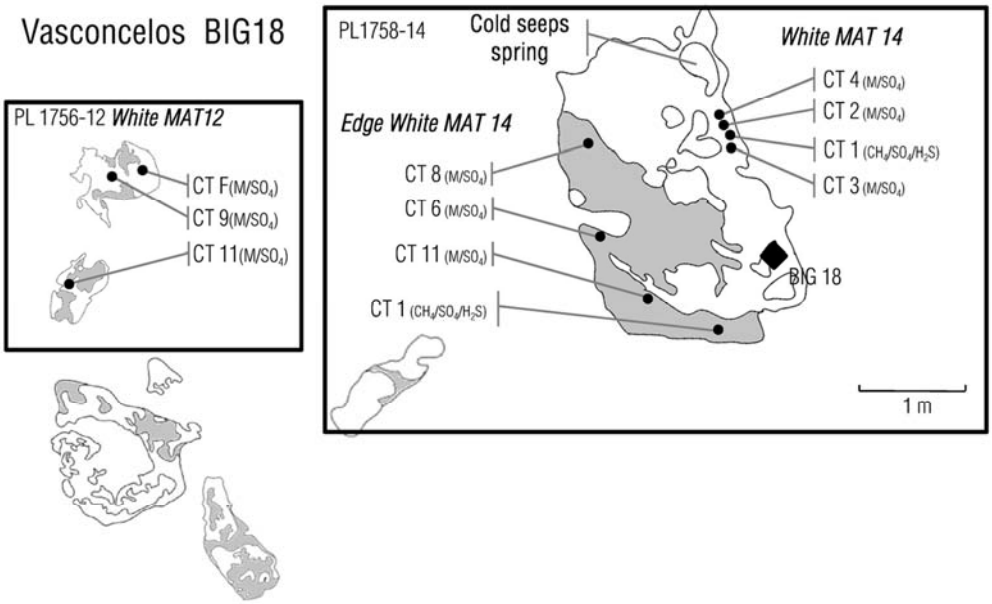

Schematic view of sampling sites around markers BIG18 (N 27°35.5781; W 111°28.9848) with *Nautile* dives areas (PL), relative position of push cores (CT, Diameter 5 cm, length 30 cm) and their geochemical measurements (CH4 for methane concentrations, SO4 for sulfate and H2S for sulfide) and microbiological analysis (M). Scale is 1 meter. Modified from Vigneron et al., 2013.
102x62mm (300 x 300 DPI)

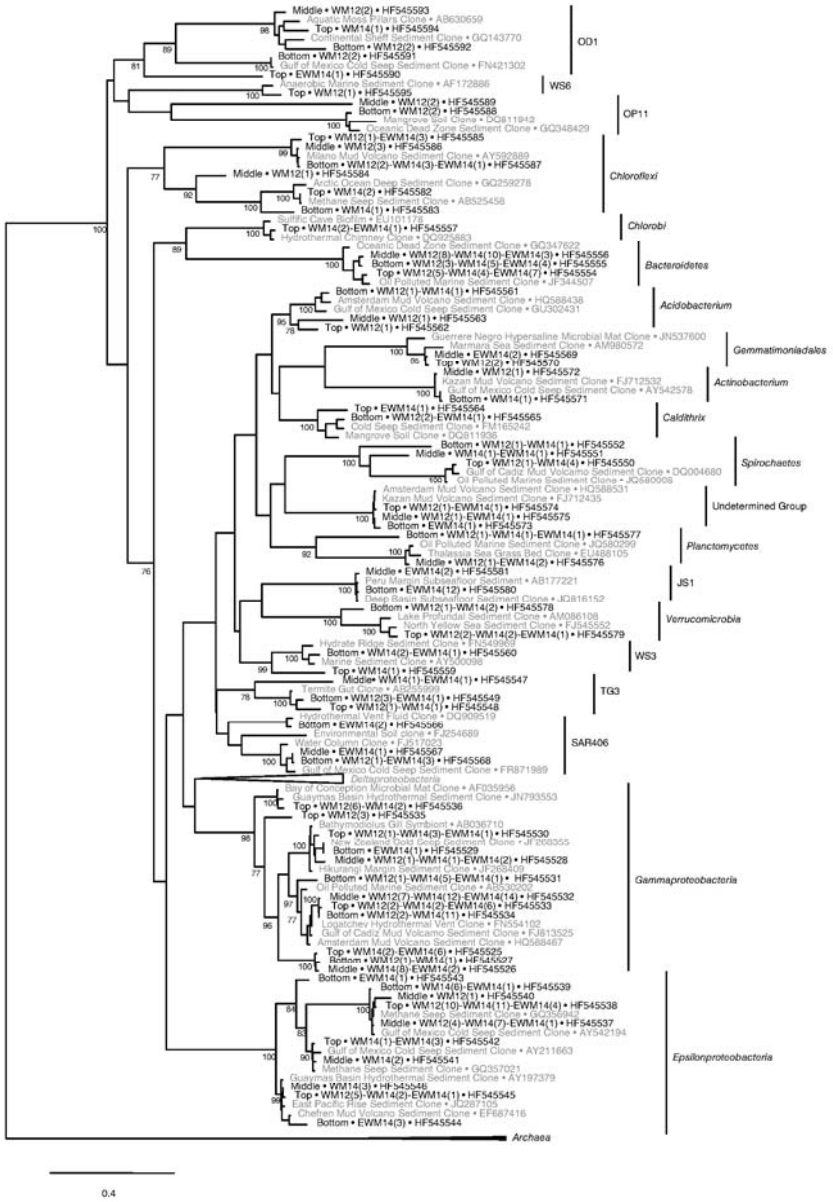

Maximum Likelihood phylogenetic tree of the bacterial 16S cDNA sequences in the Guaymas Basin cold seep sediments, performed using RAxML 7.2.8 and GTRCAT model approximation with 1000 replicates. Only bootstrap values above 70 % are shown. The scale bar indicates five substitutions per 100 nucleotides. Sequences amplified from sections 0 to 4 cmbsf are labeled "Top", sequences from 4 to 6 cmbsf are "Middle" and sequences from 8 cmbsf to the end of the core are tagged "Bottom". Only one representative sequence is shown. Number in brackets indicate the number of similar clones (above 97% similarity). White MAT12, WM12; White MAT14, WM14; EWM14, Edge of White MAT14.
176x252mm (300 x 300 DPI)

Table 1

Name	**Target group**	**Sequence (5' - 3')**	**Amplicon size (bp)**	**Annealing Temp. (°C)**	**Primer conc. (mM)**	**Maching Efficiency (%)**[a]	**Potential false-positive**
DSS-649F DSS-808R	Desulfosarcinales/ Desulfococcales group	ACT-TGA-GTA-TGG-GAG-AGG-GAA-G ACC-TAG-TGT-TCA-CCG-TTT-ACT-GC	180	60	1	72.6 51.8	None
DBB-649F DBB-808R	*Desulfobulbus* group	GCT-TGA-GTA-TGG-GAG-GGG-A CAC-CTA-GTT-CTC-ATC-GTT-TAC-AGC	180	60	1	86.6 86.6	None
SRB2-649F SRB2-808R	SEEP SRB-2 group	ACT-TGA-GTA-CCG-GAG-AGG-GA CCT-AGT-GCC-CAT-CGT-TTA-GG	180	60	1	83.8 88.3	Myxococcales and DTB120
JS1-648F JS1-730R	Candidate Division JS1	GAC-TTG-AGG-TTA-GAA-GAG-GAA-AGT-G GAG-ATA-GAC-CAG-AAA-GCC-GC	102	60	1.1	30.9 65.9	None

[a]Ratio (%) of number of organisms matched with the corresponding primer of the target group to number of all organisms of the group in the Silva SSU database (ref1200 108). The ratios were analyzed by the ARB program

Table 2

Name	**Target group**	**Sequence (5' - 3')**	**Formamide (%)**	**Ref.**
Eub338	*Bacteria*	GCT-GCC-TCC-CGT-AGG-AGT	35	(Amann et al 1990)
Arch915	*Archaea*	GTG-CTC-CCC-CGC-CAA-TTC-CT	35	(Amann et al 1990)
ANME1-350	ANME-1	AGT-TTT-CGC-GCC-TGA-TGC	40	(Boetius et al 2000)
ANME2c-622	ANME-2c	CCC-TTG-GCA-GTC-TGA-TTG	50	(Knittel et al 2009)
ANME2a-647	ANME-2a	TCT-TCC-GGT-CCC-AAG-CCT	50	(Knittel et al 2009)
DSS-658	Desulfosarcinales/ Desulfococcales	TCC-ACT-TCC-CTC-TCC-CAT	50	(Manz et al 1997)
DBB-660	*Desulfobulbus*	GAA-TTC-CAC-TTT-CCC-CTC-TG	60	(Devereuz et al 1992)
SEEP-SRB4	SEEP SRB-4	CCC-CCT-CCA-GTA-CTC-AAG	20	(Schreiber et al 2010)
SEEP2-658	SEEP SRB-2	TCC-ACT-TCC-CTC-TCC-GGT	45	(Kleindienst et al 2012)
GAM42a	*Gammaproteoacteria*	GCC-TTC-CCA-CAT-CGT-TT	35	(Manz et al 1992)